

Numerical Integration of the Fluctuating Hydrodynamic Equations

Alejandro L. Garcia,^{1,2} M. Malek Mansour,^{1,2} George C. Lie,¹
and Enrico Clementi¹

Received November 10, 1986

An approach to numerically integrate the Landau-Lifshitz fluctuating hydrodynamic equations is outlined. The method is applied to one-dimensional systems obeying the nonlinear Fourier equation and the full hydrodynamic equations for a dilute gas. Static spatial correlation functions are obtained from computer-generated sample trajectories (time series). They are found to show the emergence of long-range behavior whenever a temperature gradient is applied. The results are in very good agreement with those obtained from solving the correlation equations directly.

KEY WORDS: Fluctuating hydrodynamics; stochastic partial differential equations; nonequilibrium statistical mechanics; numerical methods.

1. INTRODUCTION

The introduction of high-speed computers has undoubtedly added a new dimension to the physics of fluids.⁽¹⁾ Numerical simulations often bridge the gap between theoretical analysis and laboratory experiments. Most computational work in hydrodynamics may be classified as strictly microscopic or macroscopic. The microscopic simulations trace the trajectories of interacting particles, while macroscopic algorithms integrate transport equations (typically PDEs) for selected initial and boundary conditions. The problem at hand dictates the choice of the simulation method.

Landau-Lifshitz fluctuating hydrodynamics is a stochastic formulation

¹ IBM Corp., Kingston, New York 12401.

² Permanent address: Service de Chimie Physique II, Université Libre de Bruxelles, 1050 Bruxelles, Belgium.

of standard fluid mechanics.⁽²⁾ Spontaneous fluctuations of hydrodynamic variables are introduced into the transport equations by adding random components to the pressure and heat fluxes. Since these fluxes are not conserved quantities, the correlations of the random terms are expected to be short-ranged and short-lived, so that at hydrodynamic scales they are assumed to be Dirac-delta-correlated. Their strengths are then chosen to yield the correct equilibrium thermodynamic fluctuations as derived from the Gibbs distribution. There are various ways of deriving the Landau-Lifshitz fluctuating hydrodynamics and there is general agreement about its validity, at least in near-equilibrium situations (for a review see Ref. 3). Extension of the theory to nonequilibrium systems leads to predictions of the asymmetry of the Brillouin lines in a liquid subjected to a constant heat flux.⁽⁴⁻⁷⁾ Kinetic theory provides further support for these predictions.^(8,9) Although these theoretical results are in agreement with light scattering experiments,^(10,11) the importance of the nonlinearities⁽¹²⁾ and the influence of the boundaries⁽¹³⁾ remain under discussion (see also Ref. 14). In fact, since the fluctuating hydrodynamic equations can be solved *analytically* for only a few elementary idealized nonequilibrium cases, in general one is forced to introduce simplifying assumptions, which need to be tested. Technological constraints have limited the quantity of available experimental data for real systems. Molecular dynamics simulations prove to be too slow and have thus far yielded only qualitative results.⁽¹⁵⁾ In this respect, the Boltzmann Monte Carlo particle simulations^(16,17) are useful because of their great computational speed, although they are restricted to dilute gas systems. An alternative approach is the direct *numerical* integration of the stochastic transport equations.

In this paper, we outline the construction of an algorithm for numerically integrating the fluctuating hydrodynamic equations. There are two complications not encountered in the usual fluid mechanics computations. The obvious one is the introduction of the stochastic fluxes. The problem is more involved than the similar Langevin problem of Brownian dynamics because our white noise process is a flux (appearing behind a spatial derivative), as opposed to a simple stochastic force.⁽¹⁸⁾ Furthermore, the space discretization of stochastic partial differential equations cannot be arbitrary; in fact, different discretization schemes may yield different answers. Second, the specification of the boundary conditions for the fluctuating quantities is nontrivial, especially if we have conserved quantities.⁽¹⁹⁾ Thus, it is crucial that we compare our results with known solutions of the fluctuating hydrodynamic equations.

In Section 2, we solve analytically the fluctuating nonlinear Fourier equation to obtain the equal-time spatial correlation function for the temperature fluctuations. The construction of the Langevin simulation

algorithm for this model is outlined in Section 3. Similarly, the more complex dilute gas equations are treated in Sections 4 and 5. We close with a general discussion of the method in Section 6.

2. NONLINEAR FOURIER EQUATION. THEORY

Consider a liquid between two parallel walls maintained at different temperatures. In the fluctuating hydrodynamic literature this problem has received considerable attention.⁽⁴⁻¹⁴⁾ Most calculations concentrate on computing the density-density dynamical correlation function, since it is directly measurable by light scattering.⁽²⁰⁾ We instead consider temperature-temperature static correlations and restrict ourselves to high-Prandtl number fluids. By this we mean that we take the temperature equation to be decoupled from the density and velocity equations. Moreover, we take the macroscopic density to be constant throughout the fluid, thus neglecting any temperature dependence it might have. We choose this example because it is exactly soluble and also because its solution is qualitatively similar to that of the more complex model considered later. Under the above assumptions, the energy conservation equation reduces to

$$\rho_0 c_v \frac{\partial}{\partial t} T = \nabla \kappa(T) \cdot \nabla T - \nabla \cdot \mathbf{g} \quad (1)$$

where ρ_0 is the mass density, c_v the heat capacity per unit mass at fixed volume, and κ the (temperature-dependent) heat conductivity coefficient. The fluctuating part of the heat flux \mathbf{g} is assumed to be a Gaussian white noise. It is zero on average and its correlation functions are given by⁽²⁾

$$\langle g_i(\mathbf{r}, t) g_j(\mathbf{r}', t') \rangle = 2\kappa_0 k_B T_0^2 \delta(\mathbf{r} - \mathbf{r}') \delta(t - t') \delta_{ij}^{K^r} \quad (2)$$

where $\kappa_0 \equiv \kappa(T_0)$ and k_B is the Boltzmann constant. The subscript 0 refers to *macroscopic* quantities, while the subscripts i, j refer to spatial components. Since the noise term is small (typically $1/\sqrt{N}$, where N is the number of particles in a macroscopic "fluid point"⁽²⁾), the deviations of the fluctuating temperature with respect to $T_0(\mathbf{r})$ (most probable path) are also small,^(21,22) so that we can linearize Eq. (1) around $T_0(\mathbf{r})$ to get

$$\frac{\partial}{\partial t} \delta T = \frac{1}{\rho_0 c_v} \nabla^2 \kappa_0 \delta T - \frac{1}{\rho_0 c_v} \nabla \cdot \mathbf{g} \quad (3)$$

In deriving the above equation we use the fact that κ depends only on temperature, so that $\delta \kappa = (\partial \kappa_0 / \partial T_0) \delta T$ and $\delta \kappa_0 / \partial \mathbf{r} = (\partial \kappa_0 / \partial T_0) (\partial T_0 / \partial \mathbf{r})$.

Because the transport coefficient and the noise are both space-dependent and because we are dealing with a finite system, it is no longer possible to use elementary transform methods (note that for small gradients, an expansion in the wavenumber of the gradient can still be used^(5,23)). To obtain the equal-time spatial correlation of the fluctuations, we employ the following identity. Given

$$\frac{d}{dt} c_i = f_i(c_1, \dots, c_n) + F_i(t), \quad i = 1, 2, \dots, n \quad (4a)$$

where the f_i are arbitrary analytic functions of the c_i , and the $F_i(t)$ are multi-Gaussian white noise processes with covariances

$$\langle F_i(t) F_j(t') \rangle = Q_{ij} \delta(t - t') \quad (4b)$$

then

$$\langle c_i(t) F_j(t') \rangle = \begin{cases} \frac{1}{2} Q_{ij}; & t = t' \\ 0; & t < t' \end{cases} \quad (4c)$$

For finite n , this identity is easily proved by writing the Fokker-Planck equation corresponding to (4a) and deriving from it the second moment equations. A comparison with the second moment equations derived directly from (4a) then leads to the relation (4c). These relations remain valid for $n \rightarrow \infty$, although, from a strictly mathematical point of view, some special care is needed in the continuum case.⁽²⁴⁾

Using the relations (4a)–(4c) and the identity

$$2\nabla_r \cdot \nabla_r f(\mathbf{r}) \delta(\mathbf{r} - \mathbf{r}') = -\{\nabla_r^2 + \nabla_{r'}^2\} f(\mathbf{r}) \delta(\mathbf{r} - \mathbf{r}') + \delta(\mathbf{r} - \mathbf{r}') \nabla_r^2 f(\mathbf{r}) \quad (5)$$

one finds

$$\begin{aligned} \frac{\partial}{\partial t} \langle \delta T(\mathbf{r}) \delta T(\mathbf{r}') \rangle &= \frac{1}{\rho_0 c_v} \{\nabla_r^2 \kappa_0 + \nabla_{r'}^2 \kappa'_0\} \langle \delta T(\mathbf{r}) \delta T(\mathbf{r}') \rangle \\ &\quad + \frac{k_B}{\rho_0^2 c_v^2} \delta(\mathbf{r} - \mathbf{r}') \nabla^2 \kappa_0 T_0^2 \end{aligned} \quad (6)$$

where $\kappa'_0 \equiv \kappa(T_0(\mathbf{r}'))$ and we have introduced the notation $\langle \delta T \delta T' \rangle$ to express the correlation function with its local equilibrium component removed:

$$\langle \delta T(\mathbf{r}) \delta T(\mathbf{r}') \rangle \equiv \langle \delta T(\mathbf{r}) \delta T(\mathbf{r}') \rangle - \frac{k_B T_0^2}{\rho_0 c_v} \delta(\mathbf{r} - \mathbf{r}') \quad (7)$$

The solution of $\langle \delta T \delta T' \rangle$ at the steady state ($\partial/\partial t \langle \delta T \delta T' \rangle_{ss} = 0$) is reduced to a classic Green's function problem. For simplicity, we assume the geometry illustrated in Fig. 1. The system is periodic in the x and z directions with walls in the planes $y=0$ and $y=L$. These walls act as infinite reservoirs, so that by fixing their temperatures, one can impose the desired heat flux across the system. The boundary conditions in the y direction are

$$T_0(x, y=0, z) = T_a; \quad T_0(x, y=L, z) = T_b \quad (8a)$$

If, moreover, we assume that the state of the system is statistically independent with respect to the walls, then the boundary conditions for δT read

$$\delta T(x, y=0, z) = \delta T(x, y=L, z) = 0 \quad (8b)$$

In fact, one can always consider an enlarged description in which the state of the walls is included as well. The evolution is then governed by a global probability density which factorizes into system variables and wall variables. Averaging over the wall variables leaves one with a stochastic process for the system variables only. A straightforward change of variables then leads to the relations (8b). Note that this is in no way contradictory with the fact that the wall variables can also be considered as fluctuating variables, as is usually done in computer experiments (stochastic boundary conditions).

The macroscopic steady-state temperature profile is given by the solution of

$$\nabla \cdot \kappa(T_0) \nabla T_0 = 0 \quad (9)$$

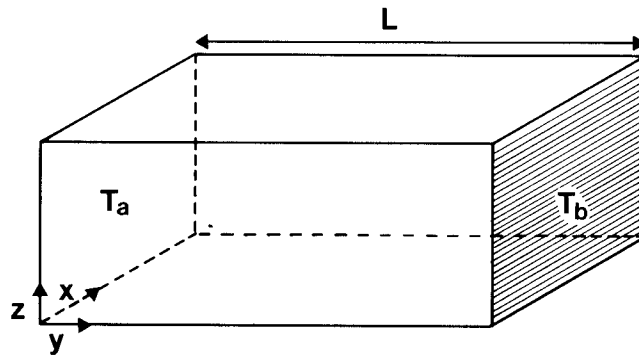


Fig. 1. Schematic representation of the system geometry.

subject to the boundary conditions (8a). To proceed further, we need to fix the analytic dependence of κ_0 with respect to T_0 . Let us assume that the thermal conductivity is of the form $\kappa(T) = \kappa_c T^\alpha$, where κ_c is a constant [the solution of Eq. (6) for constant κ is given in Ref. 25]. The steady-state temperature, from Eq. (9), is then

$$T_0(y) = [(T_b^{\alpha+1} - T_a^{\alpha+1}) y/L + T_a^{\alpha+1}]^{1/(\alpha+1)} \quad (10)$$

Since the system is periodic in x and z directions, it is useful to introduce reduced quantities defined as

$$\delta\tilde{A}(y) \equiv \frac{1}{S} \int_0^{L_x} dx \int_0^{L_z} dz \delta A(x, y, z) \quad (11)$$

where A is any dynamical variable and $S \equiv L_x L_z$ is the wall cross section (note that the reduced variables are in fact the zero-wavevector values of the "parallel" Fourier components of the dynamical variables). By standard techniques, we find the solution to be

$$\langle \delta\tilde{T} \delta\tilde{T}' \rangle_{ss} = \frac{k_B(1 + \alpha/2)}{\rho_0 c_v S L} \frac{(\kappa_0 \partial T_0 / \partial y)^2}{\kappa_0 \kappa_0'} \begin{cases} y(L - y'), & y < y' \\ y'(L - y), & y > y' \end{cases} \quad (12)$$

which is clearly proportional to the square of the imposed temperature gradient. Figure 2 shows $\langle \delta\tilde{T} \delta\tilde{T}' \rangle_{ss}$ for $y' = L/2$ (solid line); note its long-range behavior with an approximately linear decay (exactly linear if $\alpha = 0$).⁽²⁵⁾

3. NONLINEAR FOURIER EQUATION. LANGEVIN SIMULATION

We shall illustrate the simulation method by considering the linearized equation (3) after it has first been integrated over the x and z directions as defined by Eq. (11). The starting point of our Langevin simulation is its discretization in space by central differences. Because the equation is strictly parabolic, the space discretization does not give rise to any of the complications mentioned in the introduction. We again take the one-dimensional geometry illustrated in Fig. 1 and restrict our attention to the reduced temperature function $\delta\tilde{T}$. The system is divided into a one-dimensional chain of N cells plus two extra cells, one at each end, which serve to represent the walls, so that the cell length is $\lambda = L/(N+1)$. The time derivative is discretized in the increment Δt and we use the stochastic Euler scheme to integrate the equation forward in time. Higher order methods can be used, but, as pointed out by Rumelin,⁽²⁶⁾ they generally do not give

better results. Accordingly, we approximate $\delta\tilde{T}(y, t)$ as $\delta\tilde{T}_{i,n}$, where $y = i\lambda$ and $t = n\Delta t$. The trajectory $\delta\tilde{T}_{i,n}$ is computed as

$$\delta\tilde{T}_{i,n+1} = \delta\tilde{T}_{i,n} + \frac{\Delta t}{\lambda^2 \rho_0 c_v} (\kappa_{i+1} \delta\tilde{T}_{i+1,n} + \kappa_{i-1} \delta\tilde{T}_{i-1,n} - 2\kappa_i \delta\tilde{T}_{i,n}) + \frac{1}{\rho_0 c_v} \Delta F_{i,n} \quad (13)$$

where $\Delta F_{i,n}$ is an N -dimensional Gaussian distributed random vector with covariances

$$\begin{aligned} \langle \Delta F_{i,n} \Delta F_{j,m} \rangle = & \frac{k_B \Delta t}{V_c \lambda^2} \delta_{n,m}^{\text{Kr}} \{ (\kappa_{i+1} T_{i+1}^2 + \kappa_{i-1} T_{i-1}^2 + 2\kappa_i T_i^2) \delta_{i,j}^{\text{Kr}} \\ & - (\kappa_{i+1} T_{i+1}^2 + \kappa_i T_i^2) \delta_{i+1,j}^{\text{Kr}} - (\kappa_{i-1} T_{i-1}^2 + \kappa_i T_i^2) \delta_{i-1,j}^{\text{Kr}} \} \end{aligned} \quad (14)$$

and where $T_j \equiv T_0(y = j\lambda)$, $\kappa_j \equiv \kappa(T_j)$, and V_c is the cell volume. Note that to avoid cumbersome notation we have dropped the subscript zero with the understanding that κ_i and T_i are, respectively, the macroscopic value of thermal conductivity and temperature evaluated at the grid point i . The discretized form of the noise correlation, Eq. (14), may be obtained from identity (5) or by discretizing $\partial^2/\partial y \partial y'$ directly.⁽²⁷⁾ The simplest way to generate $\Delta F_{i,n}$ is to generate at each time step a vector \mathbf{R} of independent Gaussian distributed random numbers with covariances

$$\langle R_i^2 \rangle = \frac{k_B \Delta t}{V_c \lambda^2} (\kappa_{i+1} T_{i+1}^2 + \kappa_i T_i^2) \quad (15)$$

and $\langle R_i R_j \rangle = 0$ for all $i \neq j$, and then construct the discrete stochastic force as $\Delta F_{i,n} = R_i - R_{i-1}$, which can be shown to possess the desired correlation, Eq. (14).

In discretized form, the boundary conditions for δT are $\delta T_{0,n} = \delta T_{N+1,n} = 0$. The boundary cells 0 and $N+1$ represent walls held at fixed temperatures. Though their temperatures are fixed, there is still a random flux between the boundary cells and their adjacent cells in the bulk, 1 and N . As such, Eq. (14) specifies the stochastic force for all cells in the system; it is not modified for cells 1 and N . This fixes our boundary conditions for the stochastic fluxes at the walls.

A FORTRAN program was written to integrate $\delta T_{i,n}$ in time and to compute the spatial correlation function from the resulting trajectory. The program was run in parallel on two Floating Point System 264 array processors on the ICAP2 system at IBM Kingston. A system of 20 cells was integrated first for 10 million time steps and then continued for another 90 million steps. In Fig. 2 we plot two correlation functions $\langle \delta T \delta T \rangle_{ss}$ as

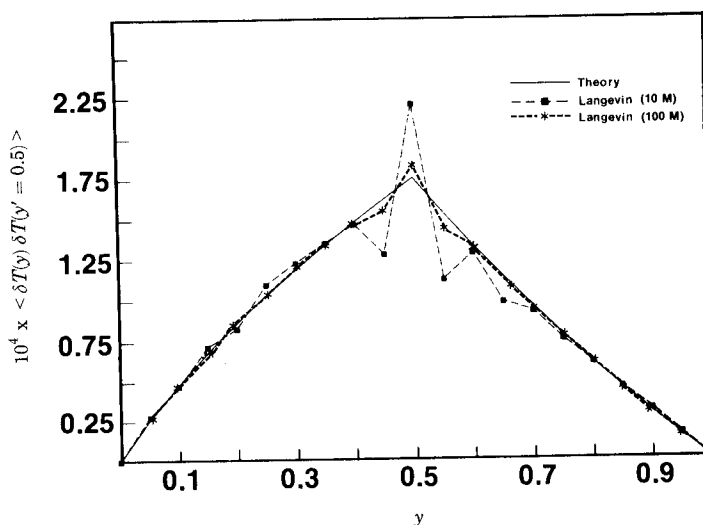


Fig. 2. Temperature-temperature static correlation function $\langle \delta T(y) \delta T(y' = L/2) \rangle_{ss}$ for the nonlinear Fourier equation. The parameters used are $\rho_0 c_v / k_B = 65$, $\alpha = 1/2$, $T_a = 2$, $T_b = 8$, $S = 1000$, $L = 1$. (—) The result from Eq. (12); (---) the correlations constructed from the trajectory of simulation with 10^7 and 10^8 time steps.

computed from the trajectory of these runs (dashed lines) and compare the results with Eq. (12) (solid line). We find excellent agreement, except for an overshoot at the peak, which is found to decay very slowly with the amount of statistics used. Note that the local equilibrium delta function contribution to $\langle \delta T_i \delta T_i \rangle$ is more than an order of magnitude larger than the nonequilibrium part of the correlation function, which may explain the difficulty in eliminating the overshoot. This situation improves somewhat when a larger number of cells is used.

We also investigated the influence of nonlinearities in the Fourier equation. To this end, we integrated the fluctuating temperature equation (1) without linearizing about T_0 for a one-dimensional system. Figure 3 shows the average temperature as compared to the deterministic one. The deviations are less than 0.01%, but they are all negative, i.e., $T_0(y)$ is strictly less than $\langle T(y) \rangle$. This is due to the asymmetry of the probability density of T , since the possible values of temperature range from zero to infinity. The average value of T therefore lies always to the right of the peak of the probability (recall that T_0 is defined as the most probable temperature). The correlation functions obtained here show better agreement with the (linearized) theory, in the sense that the overshoot observed is smaller by a factor of 2.5 for the same amount of statistics. We are not able to find a simple theoretical explanation for this observation. Suffice it to

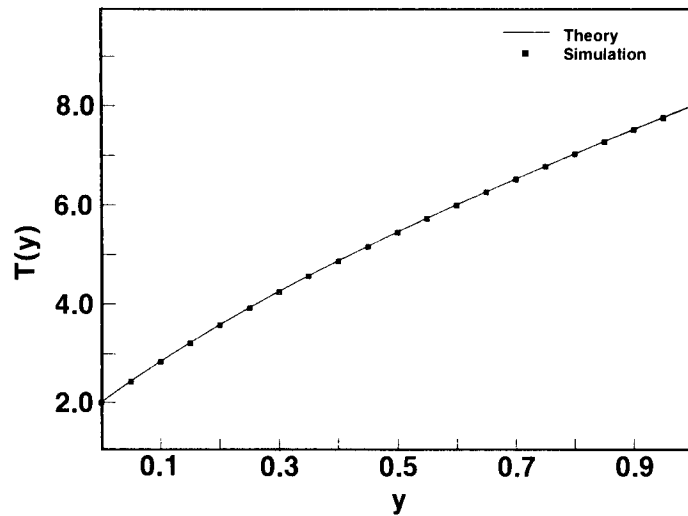


Fig. 3. Temperature profile obtained from the one-dimensional nonlinear Fourier equation. See legend to Fig. 1 for the parameters used.

say that using the full nonlinear equation does not induce any abnormal behavior. In the last section we discuss the importance of this point in more detail.

4. DILUTE GAS EQUATIONS. THEORY

Having demonstrated the method on a simple case, we move on to a more complex situation. We retain our simple geometry (Fig. 1), but with a dilute gas between the plates. As before, these plates act as infinite reservoirs, so that by fixing their temperature one can impose the desired heat flux across the system. As can be checked easily from the macroscopic hydrodynamic equations, at the stationary state the heat flux is constant and the velocity is zero. Note that we do not consider external fields, such as gravity, and therefore no convective instability can occur. Linearizing the resulting equations around the macroscopic stationary state, one obtains

$$\frac{\partial}{\partial t} \delta \rho = -\nabla \cdot \rho_0 \delta \mathbf{u} \quad (16)$$

$$\rho_0 \frac{\partial}{\partial t} \delta u_i = -\frac{\partial}{\partial x_i} \delta P + \frac{\partial}{\partial x_j} \eta_0 \left(\frac{\partial}{\partial x_i} \delta u_j + \frac{\partial}{\partial x_j} \delta u_i - \frac{2}{3} \delta_{ij}^{\kappa} \frac{\partial}{\partial x_l} \delta u_l \right) - \frac{\partial}{\partial x_j} S_{ij} \quad (17)$$

$$\frac{3}{2} \rho_0 R \frac{\partial}{\partial t} \delta T = -\frac{3}{2} R \rho_0 \delta \mathbf{u} \cdot \nabla T_0 - P_0 \nabla \cdot \delta \mathbf{u} + \nabla^2 \kappa_0 \delta T - \nabla \cdot \mathbf{g} \quad (18)$$

with the covariances of the random stress tensor S_{ij} given by

$$\begin{aligned} & \langle S_{ij}(\mathbf{r}, t) S_{kl}(\mathbf{r}', t') \rangle \\ & = 2k_B \eta_0 T_0 \left(\delta_{ik}^{\text{Kr}} \delta_{jl}^{\text{Kr}} + \delta_{il}^{\text{Kr}} \delta_{jk}^{\text{Kr}} - \frac{2}{3} \delta_{ij}^{\text{Kr}} \delta_{kl}^{\text{Kr}} \right) \delta(\mathbf{r} - \mathbf{r}') \delta(t - t') \end{aligned} \quad (19)$$

and $\langle g_i g_j \rangle$ given by Eq. (2). Here m , ρ , \mathbf{u} , and P are particle mass, mass density, velocity, and pressure, respectively, and $R \equiv k_B/m$. As before, the indices i and j in Eq. (17) refer to spatial components and the subscript zero indicates macroscopic quantities. The convention of summation over repeated indices is used. The shear viscosity η and the thermal conductivity κ are both state-dependent; note that the bulk viscosity is zero for a dilute gas. In writing the above equations we have made use of the closure relations for a dilute gas: $P(\rho, T) = R\rho T$ and $e(\rho, T) = \frac{3}{2}\rho RT$, where e is the internal energy density.

If the force between the particles is purely repulsive and obeys a power law, then the transport coefficients are only functions of temperature as⁽²⁸⁾ $\eta(T) = \eta_c T^\alpha$ and $\kappa(T) = \kappa_c T^\alpha$. For a hard sphere gas, the exponent α is one-half, and, from Chapman-Enskog theory, $\kappa_c/\eta_c = 15R/4$.

In our geometry, the macroscopic values of density and temperature are determined from

$$\frac{\partial}{\partial y} P_0 = \frac{\partial}{\partial y} R\rho_0 T_0 = 0 \quad (20)$$

and Eq. (9). The temperature is again given by Eq. (10) and the density is P_0/RT_0 , where the pressure P_0 is constant throughout the system.

Since we are mainly interested in the influence of nonequilibrium constraints, we shall again limit ourselves to reduced quantities, defined by Eq. (11). The equations for the reduced x and z components of the velocity now decouple from the rest. These components are not influenced by the constraint and it is easy to check that their static correlation functions are given by their local equilibrium expressions. We instead concentrate on the remaining equations for the reduced density $\delta\rho$, y velocity δv , and temperature δT ,

$$\frac{\partial}{\partial t} \delta\rho = -\frac{\partial}{\partial y} \rho_0 \delta v \quad (21)$$

$$\rho_0 \frac{\partial}{\partial t} \delta v = -R \frac{\partial}{\partial y} (T_0 \delta\rho + \rho_0 \delta T) + \frac{4}{3} \frac{\partial}{\partial y} \eta_0 \frac{\partial}{\partial y} \delta v - \frac{\partial}{\partial y} S_{yy} \quad (22)$$

$$\frac{3}{2} \rho_0 R \frac{\partial}{\partial t} \delta T = -\frac{3}{2} R \rho_0 \delta v \frac{\partial}{\partial y} T_0 - P_0 \frac{\partial}{\partial y} \delta v + \frac{\partial^2}{\partial y^2} \kappa_0 \delta T - \frac{\partial}{\partial y} g_y \quad (23)$$

The covariances of the reduced noises are

$$\langle S_{yy}(y, t) S_{yy}(y', t') \rangle = \frac{8}{3} k_B T_0 \frac{\eta_0}{S} \delta(y - y') \delta(t - t') \quad (24a)$$

$$\langle g_y(y, t) g_y(y', t') \rangle = 2k_B T_0^2 \frac{\kappa_0}{S} \delta(y - y') \delta(t - t') \quad (24b)$$

$$\langle S_{yy}(y, t) g_y(y', t') \rangle = 0 \quad (24c)$$

There remains the specification of the boundary conditions for the above equations. The boundary conditions for δT are the same as in Section 2, namely

$$\delta T(y=0, t) = \delta T(y=L, t) = 0 \quad (25)$$

The boundary condition for δv follows from the conservation of the total number of particles:

$$\int_0^L \delta \rho(y, t) dy = 0 \quad \forall t \quad (26)$$

Inserting (26) into the continuity equation, one finds

$$\rho_0(y) \delta v(y)|_{\text{boundaries}} = 0 \quad (27)$$

In words, the containing walls are rigid. This completes our specification of the boundary conditions.

It may seem strange that we do not have to specify any boundary conditions for $\delta \rho$. From a physical point of view, this comes from the fact that the state of the wall can only constrain the temperature and velocity of the gas at the wall, whereas the behavior of the density close to the wall is entirely determined by the internal dynamics of the system. From the mathematical point of view, it can be shown that for any given initial conditions ($\delta \rho(y, 0)$, $\delta \mathbf{u}(y, 0)$, $\delta T(y, 0)$), the boundary conditions for $\delta \mathbf{u}$ and δT are sufficient to specify completely the solution of the system.⁽¹⁹⁾

Having set the stage, one might proceed as in Section 2 to derive the evolution equations for the correlations of the fluctuations. Since the derivation is straightforward, we omit the details. We simply mention that the resulting equations have not yielded any closed analytic solutions. The correlation equations may, however, be solved numerically; for the steady-state solution the space-discretized versions of these equations may be solved by standard techniques.⁽¹⁷⁾ Some of the results obtained with this method will be discussed in the next section. The advantages and limitations of this approach *vis à vis* Langevin simulation are discussed in Section 6.

5. DILUTE GAS EQUATIONS. LANGEVIN SIMULATION

The first step in the construction of the Langevin simulation is the space discretization of Eqs. (21)–(23). This is not trivial, since different discretization schemes may lead to different answers. These differences arise from the fact that the hydrodynamic variables are, in equilibrium, Dirac-delta-correlated in space. These local equilibrium components persist out of equilibrium, confronting us with the problem of discretizing generalized functions. The problem is reminiscent of the well known Ito–Stratonovich calculation for multiplicative noise processes.⁽¹⁸⁾ To overcome this difficulty, we shall again use (4a)–(4c) to derive the static correlation functions, which will assist us in determining the best discretization scheme. The details of the formulation may be found in the Appendix; suffice it to say that it is possible to formulate the evolution equations in such a way that one always obtains the same correlation equations regardless of the stage at which the equations are discretized. This guarantees that at least the correlation functions are given correctly.

The boundary value problem for the discretized equations also requires a careful treatment, mainly because of the conservation-of-mass condition. For example, consider the continuity equation (21) discretized in space by central differences,

$$\frac{\partial}{\partial t} \delta\rho_i = -\frac{1}{2\lambda} (\rho_{i+1} \delta v_{i+1} - \rho_{i-1} \delta v_{i-1}) \quad (28)$$

with the mass conservation condition

$$\sum_{i=1}^N \delta\rho_i = 0 \quad (29)$$

It is not possible to specify a suitable boundary condition for δv corresponding to Eq. (27) that guarantees condition (29), and it is easy to check that none of the simple discretization schemes (forward, backward, higher order, etc.) can resolve this problem. We instead consider a more sophisticated half-grid scheme in which the system is divided into $2N + 1$ grid points (plus two extra grid points at the walls; see Fig. 4). The velocity and temperature *fluctuations* are computed at integer grid points, while the

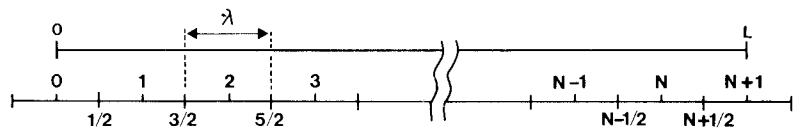


Fig. 4. Schematic representation of the half-grid spatial discretization.

density *fluctuations* are computed at half-grid points. The discretized (central-difference) continuity equation then takes the form

$$\frac{\partial}{\partial t} \delta \rho_{i+1/2} = -\frac{1}{\lambda} (\rho_{i+1} \delta v_{i+1} - \rho_i \delta v_i); \quad i=0, 1, \dots, N \quad (30)$$

with the boundary condition $\rho_0 \delta v_0 = \rho_{N+1} \delta v_{N+1} = 0$. It is now easy to check that Eq. (30) together with this boundary condition indeed conserve total mass. Analogously, the boundary condition for the temperature fluctuations is $\delta T_0 = \delta T_{N+1} = 0$. Note that in this half-grid formulation, it is not possible to specify a boundary condition for $\delta \rho$, just as it is not possible in the continuum case (see the preceding section).

The full discretized fluctuating hydrodynamic equations are given at the end of the Appendix. An important property of these discrete evolution equations is that their corresponding correlation equations yield *exactly* the equilibrium results *independent* of the number of grid points used to discretize the system.

The evolution equations for the fluctuations were numerically integrated in time and the resulting trajectory was used to compute several static correlation functions. As discussed above, the formulation of the

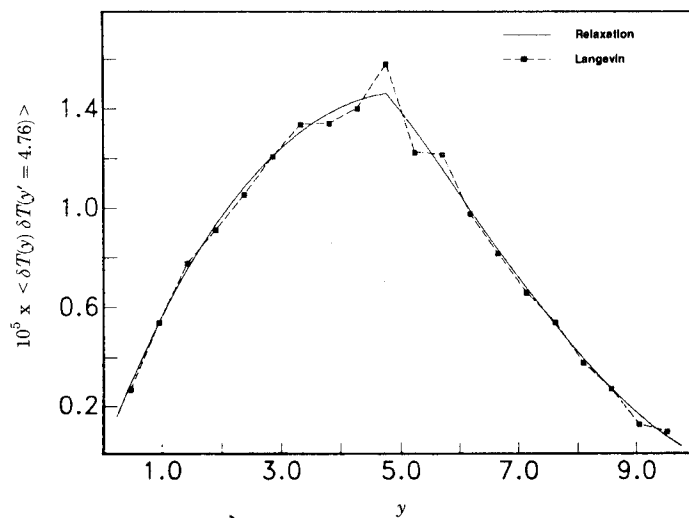


Fig. 5. Temperature-temperature static correlation function $\langle \delta T(y) \delta T(y' = 4.76) \rangle_{ss}$ for the dilute gas equations. The parameters are $\rho_0 = 200$, $\eta_c = 5\sqrt{\pi}/16$, $\alpha = 1/2$, $T_a = 1$, $T_b = 3$, $S = 1$, $L = 10\lambda$. (—) Obtained by numerically solving the correlation equations (see Ref. 17); (---) the correlation constructed from the trajectory simulation. Note that y is expressed in units of λ .

Langevin simulation was guided by the form of the correlation equations. These correlation equations can be solved numerically and the results must be equal (within the statistical error) to those constructed from the trajectory. This is a good test of the self-consistency of the method.

In Fig. 5, we present the temperature–temperature static correlation function $\langle \delta T_i \delta T_j \rangle_{ss}$ as determined by both methods. Notice the qualitative similarity with the results from the simple Fourier equation presented in Sections 2 and 3. The agreement shown in Fig. 5 is quite good, except for an overshoot at the peak. As seen in Section 3, this same phenomenon was found in the Langevin simulation of the nonlinear Fourier equation. We believe that this discrepancy is primarily due to the presence of the local equilibrium contribution to the fluctuations, which is an order of magnitude larger than the nearest neighbor correlation. This is confirmed in Fig. 6, where we depict the velocity–temperature correlation function $\langle \delta v_i \delta T_j \rangle_{ss}$, for which the local equilibrium contribution is identically zero. The results of the two methods are now in perfect agreement, clearly establishing this assertion. Note that the correlation functions show a strong dependence on the size of the system. This is illustrated in Fig. 7, where we present the temperature–temperature static correlation function $\langle \delta T_i \delta T_j \rangle_{ss}$ again, but for a larger system. These results are also in full agreement with the data from Monte Carlo Boltzmann particle simulations.⁽¹⁷⁾

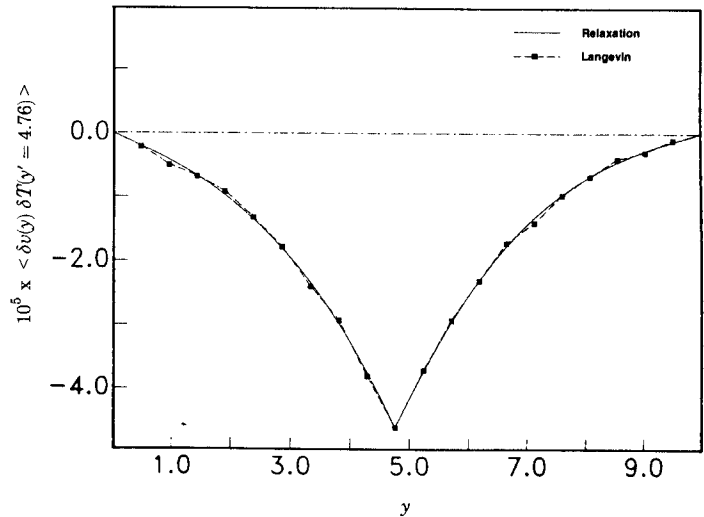


Fig. 6. The y -velocity–temperature static correlation function $\langle \delta v(y) \delta T(y' = 4.76) \rangle_{ss}$ for the dilute gas equations. See legend to Fig. 5 for details.

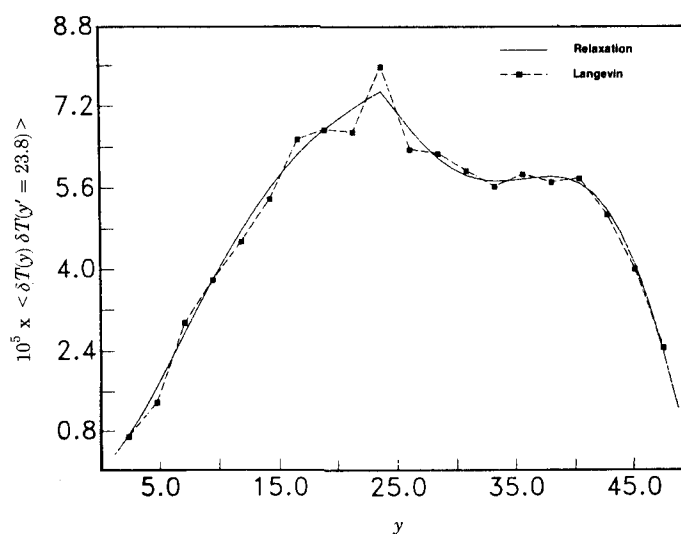


Fig. 7. Temperature-temperature static correlation function $\langle \delta T(y) \delta T(y' = 23.8) \rangle_{ss}$ for the dilute gas equations. The parameters are $\rho_0 = 400$, $\eta_c = 5\sqrt{\pi}/16$, $\alpha = 1/2$, $T_a = 1$, $T_b = 3$, $S = 1$, $L = 50\lambda$. (—) Obtained by numerically solving the correlation equations (see Ref. 17); (- -) the correlation constructed from the trajectory simulation. Comparison with the results in Ref. 17 demonstrates the agreement with dynamic Monte Carlo particle simulations. Note that y is expressed in units of λ .

6. CONCLUSIONS

It is clear that Langevin simulations are successful in describing hydrodynamic fluctuations. Their usefulness in the study of fluctuating hydrodynamics, however, would depend on their being able to treat problems that are intractable by other approaches. Though much of the work on fluctuating hydrodynamics was originally stimulated by experimental results, the current technological limitations place a considerable constraint on these laboratory measurements.^(10,11) Thus, particle simulations have been playing a central role in the theory of fluctuations over the past 15 years,³ but unfortunately even with modern supercomputers molecular dynamics studies are still limited to small systems integrated for short times.

At the level of hydrodynamic equations, a number of strategies are available; the most common is the computation of the eigenmodes of the nonequilibrium hydrodynamic operator.^(29,30) The approach illustrated in

³ See, e.g., Hoover, Evans, and others in Ref. 1.

Sections 2 and 4 yields directly the evolution equations for the equal-time correlation functions. For simple models these equations can be solved exactly; for more complex models they are amenable to numerical solution by the relaxation method. This approach, however, has two limitations.

The first is the number of grid points that may be used to discretize the system: for the dilute gas equations, we have 15 correlation equations (in $\delta\rho$, $\delta\mathbf{u}$ and δT); if our system is discretized into N cells, then we must solve $15N^2$ simultaneous equations (involving a complicated $15N^2 \times 15N^2$ matrix). Furthermore, there remains the problem of computing the dynamical correlation functions from the static correlations. The comparable Langevin simulation, however, integrates only $5N$ evolution equations. From the resulting trajectory, both static and dynamic correlations may be obtained directly. Certainly, the relaxation method converges much faster than the stochastic Langevin method for small problems. For complex problems (e.g., 2D or 3D systems), however, the relaxation approach quickly becomes computationally prohibitive.

The second, more important, limitation of the relaxation method is that the correlation equations can only be formulated from evolution equations that are linearized about a steady state. Here, we have restricted our attention to systems far from instabilities and as such this has not been a restriction. Near the instabilities, however, the nonlinear terms can no longer be neglected and of course we are interested in extending our investigation to the onset of instabilities.

It should, however, be realized that the validity of the fluctuating hydrodynamic formalism becomes questionable beyond instabilities where multiple solutions of the macroscopic hydrodynamic equations are expected. Indeed, a Langevin formalism is always characterized by a macroscopic law to which a noise term has been added. This law may be linear or nonlinear and the noise may be white or be correlated in time, but in any case, in the limit of vanishing noise, one must recover the original macroscopic law. The macroscopic behavior therefore appears as the most probable path (and not necessarily the average!) of the stochastic process so defined. This is precisely the meaning of the equilibrium statistical ensembles, where the thermodynamic quantities are some particular values of the state variables for which the entropy or some other thermodynamic potential reaches its extremum. In nonequilibrium systems, the probability density associated with the corresponding Langevin type of equations is somehow equivalent to the equilibrium partition function in the sense that the macroscopic paths are defined by a particular set of dynamical variables for which the probability density is maximum. Close to and beyond the instability, the system is generally characterized by more than one stable attractor, that is, the probability density is now multimodal.

Each local maximum characterizes a possible stable or metastable solution of the corresponding macroscopic equations. While a Langevin approach might be suitable to describe the behavior of the system around a given maximum, it seems unlikely that it would correctly describe the global behavior^(31,32) (for a more detailed discussion see also Ref. 33). Nevertheless, it seems promising that the Langevin formulation describes correctly the state of the system up to and including the bifurcation point, so that we may study the onset of hydrodynamic instabilities via the techniques developed in this paper. Such a program is currently under study.

APPENDIX. DISCRETIZATION OF THE DILUTE GAS EQUATIONS

There are many ways in which the terms in Eqs. (21)–(23) may be arranged. So long as we work with the continuous equations, all forms are equally valid. When the equations are discretized, however, this is no longer the case, because some identities that are valid for the continuous equations no longer hold for their discretized versions. Let us illustrate with an example; consider the y -velocity and temperature equations for the reduced fluctuations,

$$\frac{\partial}{\partial t} \delta v = -\frac{R}{\rho_0} \frac{\partial}{\partial y} \{ \rho_0 \delta T + T_0 \delta \rho \} + \text{dissipative terms} \quad (\text{A1})$$

$$\frac{\partial}{\partial t} \delta T = -\delta v \frac{\partial}{\partial y} T_0 - \frac{2}{3} T_0 \frac{\partial}{\partial y} \delta v + \text{dissipative terms} \quad (\text{A2})$$

The evolution equation for the velocity–temperature correlations is

$$\begin{aligned} & \frac{\partial}{\partial t} \langle \delta v \delta T' \rangle \\ &= -\langle \delta v \delta v' \rangle \frac{\partial T_0'}{\partial y'} - \frac{2}{3} T_0' \frac{\partial}{\partial y'} \langle \delta v \delta v' \rangle \\ & \quad - \frac{R}{\rho_0} \frac{\partial}{\partial y} (\rho_0 \langle \delta T \delta T' \rangle + T_0 \langle \delta \rho \delta T' \rangle) \\ & \quad - \frac{5 k_B T_0}{3 \rho_0 S} \frac{\partial T_0}{\partial y} \delta(y - y') + \text{dissipative terms} \end{aligned} \quad (\text{A3})$$

Again we employ the notation $\langle \delta a \delta b' \rangle$ to express the correlation function with the local equilibrium contribution removed; note that if a and b are different (e.g., $a \equiv \rho$ and $b \equiv T$), then $\langle \delta a \delta b' \rangle = \langle \delta a \delta b' \rangle$. Discretizing by central differences, we find that this correlation equation takes the form

$$\begin{aligned}
& \frac{\partial}{\partial t} \langle \delta v_i \delta T_j \rangle \\
&= - \langle \delta v_i \delta v_j \rangle \left(\frac{\partial T_0}{\partial y} \right)_j - \frac{2}{3} T_j \frac{1}{2\lambda} (\langle \delta v_i \delta v_{j+1} \rangle - \langle \delta v_i \delta v_{j-1} \rangle) \\
&\quad - \frac{R}{\rho_i} \frac{1}{2\lambda} (\rho_{i+1} \langle \delta T_{i+1} \delta T_j \rangle - \rho_{i-1} \langle \delta T_{i-1} \delta T_j \rangle) \\
&\quad + 2T_{i+1/2} \langle \delta \rho_{i+1/2} \delta T_j \rangle - 2T_{i-1/2} \langle \delta \rho_{i-1/2} \delta T_j \rangle) \\
&\quad - \frac{5 k_B T_i}{3 \rho_i V_c} \left(\frac{\partial T_0}{\partial y} \right)_i \delta_{ij}^{Kr} + \text{dissipative terms} \tag{A4}
\end{aligned}$$

Returning to Eqs. (A1) and (A2), if we first discretize the fluctuation equations and then use these discretized versions to compute the evolution equation for $\langle \delta v_i \delta T_j \rangle$, we find

$$\begin{aligned}
& \frac{\partial}{\partial t} \langle \delta v_i \delta T_j \rangle \\
&= - \langle \delta v_i \delta v_j \rangle \left(\frac{\partial T_0}{\partial y} \right)_j - \frac{2}{3} T_j \frac{1}{2\lambda} (\langle \delta v_i \delta v_{j+1} \rangle - \langle \delta v_i \delta v_{j-1} \rangle) \\
&\quad - \frac{R}{\rho_i} \frac{1}{2\lambda} (\rho_{i+1} \langle \delta T_{i+1} \delta T_j \rangle - \rho_{i-1} \langle \delta T_{i-1} \delta T_j \rangle) \\
&\quad + 2T_{i+1/2} \langle \delta \rho_{i+1/2} \delta T_j \rangle - 2T_{i-1/2} \langle \delta \rho_{i-1/2} \delta T_j \rangle) \\
&\quad - \frac{k_B T_i}{\rho_i V_c} \left(\frac{\partial T_0}{\partial y} \right)_i \delta_{ij}^{Kr} - \frac{1}{2\lambda} \frac{2k_B}{3V_c} (\delta_{i+1,j}^{Kr} - \delta_{i-1,j}^{Kr}) \frac{T_j}{\rho_i} (T_j - T_i) \\
&\quad + \text{dissipative terms} \tag{A5}
\end{aligned}$$

By inspection, (A4) and (A5) are not equivalent (except at equilibrium) and their solutions must differ. If, however, we rearrange the terms in (A2), we may write the temperature equation as

$$\frac{\partial}{\partial t} \delta T = - \frac{5}{3} \delta v \frac{\partial T_0}{\partial y} - \frac{2}{3} \frac{T_0}{\rho_0} \frac{\partial}{\partial y} \rho_0 \delta v + \text{dissipative terms} \tag{A6}$$

The discretized correlation equation for $\langle \delta v \delta T \rangle$ computed from (A1) and (A6) is now the same whether one discretizes initially or at the end of the calculation. In this way, we use the construction of the correlation equations as the criterion for selecting how to discretize our equations.

The final forms of the discretized fluctuating hydrodynamic equations are

$$\frac{\partial}{\partial t} \delta \rho_{i+1/2} = -\frac{1}{\lambda} (\rho_{i+1} \delta v_{i+1} - \rho_i \delta v_i) \quad (\text{A7})$$

$$\begin{aligned} \frac{\partial}{\partial t} \delta v_i = & -\frac{R}{\rho_i} \frac{1}{\lambda} (T_{i+1/2} \delta \rho_{i+1/2} - T_{i-1/2} \delta \rho_{i-1/2}) \\ & -\frac{R}{\rho_i} \frac{1}{2\lambda} (\rho_{i+1} \delta T_{i+1} - \rho_{i-1} \delta T_{i-1}) \\ & + \frac{4}{3\rho_i} \frac{1}{\lambda^2} (\eta_{i+1} \delta v_{i+1} + \eta_{i-1} \delta v_{i-1} - 2\eta_i \delta v_i) \\ & - \frac{C_\eta}{\lambda} (\rho_{i+1} \delta v_{i+1} - \rho_{i-1} \delta v_{i-1}) + \Delta F_i^v \end{aligned} \quad (\text{A8})$$

$$\begin{aligned} \frac{\partial}{\partial t} \delta T_i = & -\frac{5}{3} \delta v_i \left(\frac{\partial T_0}{\partial y} \right)_i - \frac{2}{3} \frac{T_i}{\rho_i} \frac{1}{2\lambda} (\rho_{i+1} \delta v_{i+1} - \rho_{i-1} \delta v_{i-1}) \\ & + \frac{2}{3R\rho_i} \frac{1}{\lambda^2} (\kappa_{i+1} \delta T_{i+1} + \kappa_{i-1} \delta T_{i-1} - 2\kappa_i \delta T_i) + \Delta F_i^T \end{aligned} \quad (\text{A9})$$

where

$$C_\eta \equiv \frac{1}{3} \frac{\eta_0}{\rho_0 T_0} \frac{\partial T_0}{\partial y}$$

is a constant. The variances of ΔF_i^v and ΔF_i^T are obtained from (24a)–(24c), recalling the discussion in Section 3. Explicitly, we have

$$\begin{aligned} \langle \Delta F_i^v \Delta F_j^v \rangle = & \frac{4k_B}{3\rho_i \rho_j V_c \lambda^2} \delta(t-t') \{ (\eta_{i+1} T_{i+1} + \eta_{i-1} T_{i-1} + 2\eta_i T_i) \delta_{ij}^{\text{Kr}} \\ & - (\eta_i T_i + \eta_j T_j) (\delta_{i+1,j}^{\text{Kr}} + \delta_{i-1,j}^{\text{Kr}}) \} \end{aligned} \quad (\text{A10})$$

$$\begin{aligned} \langle \Delta F_i^T \Delta F_j^T \rangle = & \frac{4k_B}{9R^2 \rho_i \rho_j V_c \lambda^2} \delta(t-t') \{ (\kappa_{i+1} T_{i+1}^2 + \kappa_{i-1} T_{i-1}^2 + 2\kappa_i T_i^2) \delta_{ij}^{\text{Kr}} \\ & - (\kappa_i T_i^2 + \kappa_j T_j^2) (\delta_{i+1,j}^{\text{Kr}} + \delta_{i-1,j}^{\text{Kr}}) \} \end{aligned} \quad (\text{A11})$$

REFERENCES

1. Special issue devoted to Nonequilibrium Fluids, *Physica* **118A** (1983).
2. L. D. Landau and E. M. Lifshitz, *Fluid Mechanics* (Pergamon Press, Oxford, 1984).
3. M. H. Ernst and E. G. D. Cohen, *J. Stat. Phys.* **25**:153 (1981).

4. I. Procaccia, D. Ronis, and I. Oppenheim, *Phys. Rev. Lett.* **42**:287 (1979); D. Ronis, I. Procaccia, and I. Oppenheim, *Phys. Rev. A* **19**:1324 (1979); D. Ronis and S. Putterman, *Phys. Rev. A* **22**:773 (1980).
5. A.-M. S. Tremblay, M. Arai, and E. Siggia, *Phys. Rev. A* **23**:1451 (1981).
6. G. Van Der Zwan, D. Bedaux, and P. Mazur, *Physica* **107A**:491 (1981).
7. T. R. Kirkpatrick, E. G. D. Cohen, and J. R. Dorfman, *Phys. Rev. Lett.* **44**:472 (1980).
8. T. R. Kirkpatrick, E. G. D. Cohen, and J. R. Dorfman, *Phys. Rev. Lett.* **42**:862 (1979).
9. J. Dufty, in *Spectral Line Shapes*, P. Wende, ed. (de Gruyter, Berlin, 1981), p. 1143.
10. D. Beysens, Y. Garrabos, and G. Zalczer, *Phys. Rev. Lett.* **45**:403 (1980); R. Penney, H. Kieft, and J. M. Clouter, *Bull. Can. Assoc. Phys.* **39**:BB8 (1983).
11. G. Wegdam, N. M. Van Keulen, and J. C. F. Michielsen, *Phys. Rev. Lett.* **55**:630 (1985).
12. T. R. Kirkpatrick and E. G. D. Cohen, *Phys. Lett.* **78A**:350 (1980); D. Ronis and I. Procaccia, *Phys. Rev. A* **26**:1812 (1982).
13. G. Satten and D. Ronis, *Phys. Rev. A* **26**:940 (1982); T. R. Kirkpatrick and E. G. D. Cohen, *Phys. Rev. A* **26**:972 (1982).
14. A. M. Tremblay, in *Recent Developments in Nonequilibrium Thermodynamics*, J. Casas-Vasquez, D. Jou, and G. Lebon, eds. (Springer-Verlag, Berlin, 1984).
15. M. Mareschal and E. Kestemont, *Phys. Rev. A* **30**:1158 (1984).
16. A. Garcia, *Phys. Rev. A* **34**:1454 (1986).
17. M. Malek Mansour, A. L. Garcia, G. C. Lie, and E. Clementi, *Phys. Rev. Lett.* **58**:874 (1987).
18. L. Arnold, *Stochastic Differential Equations: Theory and Applications* (Wiley, New York, 1974).
19. M. Malek Mansour, J. W. Turner, A. L. Garcia, M. Mareschal, and G. Nicolis, in preparation.
20. B. Berne and R. Pecora, *Dynamic Light Scattering* (Wiley, New York, 1976).
21. T. G. Kurtz, *Math. Prog. Study* **5**:67 (1976); *Huston J. Math.* **3**:67 (1977); *Stoch. Proc. Appl.* **6**:223 (1978).
22. C. VanDen Broeck, M. Malek Mansour, and F. Baras, *J. Stat. Phys.* **28**:557 (1982).
23. J. Perez-Madrid and J. M. Rubi, *Phys. Rev. A* **33**:2716 (1986).
24. L. Arnold and R. Lefever, eds., *Stochastic Nonlinear Systems in Physics, Chemistry and Biology* (Springer, Berlin, 1981); J. W. Duffy, J. J. Brey, and M. C. Marchetti, *Phys. Rev. A* **33**:4307 (1986).
25. G. Nicolis and M. Malek Mansour, *Phys. Rev. A* **29**:2845 (1984).
26. W. Rumelin, *SIAM J. Numer. Anal.* **19**:604 (1982).
27. M. Abramowitz and I. Stegun, *Handbook of Mathematical Functions*, 9th ed. (Dover, New York, 1972), Eq. 25.3.27.
28. P. Resibois and M. DeLeener, *Classical Kinetic Theory of Fluids* (Wiley, New York, 1977).
29. R. Schmitz and E. G. D. Cohen, *J. Stat. Phys.* **38**:285 (1985).
30. J. Lutsko and J. W. Dufty, *Phys. Rev. A* **32**:3040 (1985).
31. G. Nicolis and I. Prigogine, *Self-Organization in Nonequilibrium Systems* (Wiley, New York, 1977).
32. M. Malek Mansour, C. Van Den Broeck, G. Nicolis, and J. W. Turner, *Ann. Phys. (N.Y.)* **131**:283 (1981).
33. N. G. Van Kampen, *Stochastic Processes in Physics and Chemistry* (North-Holland, Amsterdam, 1981).